

Article

Not peer-reviewed version

Comparing DNA Methylation Landscapes in Peripheral Blood from Myalgic Encephalomyelitis/Chronic Fatigue Syndrome and Long COVID Patients

[Katie Peppercorn](#) , [Sayan Sharma](#) , Christina D Edgar , [Peter A Stockwell](#) , [Euan J Rodger](#) , [Aniruddha Chatterjee](#) * , [Warren P. Tate](#) *

Posted Date: 20 May 2025

doi: 10.20944/preprints202505.1582.v1

Keywords: Myalgic Encephalomyelitis/Chronic Fatigue Syndrome; Long COVID; DNA methylation; peripheral blood mononuclear cells; differentially methylated fragments; hypomethylation; hypermethylation



Preprints.org is a free multidisciplinary platform providing preprint service that is dedicated to making early versions of research outputs permanently available and citable. Preprints posted at Preprints.org appear in Web of Science, Crossref, Google Scholar, Scilit, Europe PMC.

Copyright: This open access article is published under a Creative Commons CC BY 4.0 license, which permit the free download, distribution, and reuse, provided that the author and preprint are cited in any reuse.

Disclaimer/Publisher's Note: The statements, opinions, and data contained in all publications are solely those of the individual author(s) and contributor(s) and not of MDPI and/or the editor(s). MDPI and/or the editor(s) disclaim responsibility for any injury to people or property resulting from any ideas, methods, instructions, or products referred to in the content.

Article

Comparing DNA Methylation Landscapes in Peripheral Blood from Myalgic Encephalomyelitis/Chronic Fatigue Syndrome and Long COVID Patients

Katie Peppercorn ^{1,†}, Sayan Sharma ^{2,†}, Christina D Edgar ¹, Peter A Stockwell ², Euan J Rodger ², Aniruddha Chatterjee ^{2,*} and Warren P Tate ^{2,*}

¹ Department of Biochemistry, School of Biomedical Sciences, University of Otago, Dunedin, New Zealand

² Department of Pathology, Dunedin School of Medicine, University of Otago, Dunedin, New Zealand

* Correspondence: warren.tate@otago.ac.nz; aniruddha.chatterjee@otago.ac.nz

† These authors contributed equally to the study.

Abstract: Post-viral conditions, Myalgic Encephalomyelitis/Chronic Fatigue Syndrome (ME/CFS) and Long COVID (LC), share >95% of their symptoms, but the connection between disturbances in their underlying molecular biology is unclear. This study investigates DNA methylation patterns in peripheral blood mononuclear cells (PBMC) from patients with ME/CFS, LC, and healthy controls (HC). Reduced Representation Bisulphite Sequencing (RRBS) was applied to the DNA of age- and sex-matched cohorts: ME/CFS (n=5), LC (n=5) and HC (n=5). The global DNA methylomes of the three cohorts were similar and spread equally across all chromosomes, except the sex chromosomes, but there were distinct minor changes in the exons of the disease cohorts towards more hypermethylation. A principal component analysis (PCA) analysing significant methylation changes ($p < 0.05$) separated the ME/CFS, LC and HC cohorts into three distinct clusters. Analysis with a limit of >10% methylation difference and at $P < 0.05$ identified 214 Differentially Methylated Fragments (DMF) in ME/CFS, and 429 in LC compared to HC. Of these 118 DMFs were common to both cohorts. Those in promoters and exons were mainly hypermethylated, with a minority hypomethylated. There were rarer examples with either no change in methylation in ME/CFS but a change in LC, or a methylation change in ME/CFS but in the opposite direction in LC. The differential methylation in a number of fragments was significantly greater in the LC cohort than in the ME/CFS cohort. Our data reveal a generally shared epigenetic makeup between ME/CFS and LC but with specific distinct changes. Differences between the two cohorts likely reflect the stage of the disease from onset (LC 1 year vs ME/CFS 12 years) but specific changes imposed by the SARS-CoV-2 virus in the case of the LC patients cannot be discounted. These findings provide a foundation for further studies with larger cohorts at the same disease stage and for functional analyses to establish clinical relevance.

Keywords: Myalgic Encephalomyelitis/Chronic Fatigue Syndrome; Long COVID; DNA methylation; peripheral blood mononuclear cells; differentially methylated fragments; hypomethylation; hypermethylation

1. Introduction

The COVID-19 pandemic has infected a reported ~778 million people worldwide [1], and from those have arisen an estimated 60 million cases or more of a post-viral debilitating syndrome generally referred to as Long COVID (LC) [2–4] and clinically as Post-Acute Sequelae of SARS-CoV-2 infections (PASC) [5]. This scenario is unique as cases of post-viral syndromes in the past have been ‘drip fed’ from geographically-isolated boutique infectious outbreaks, or endemic viruses in our

communities like Epstein-Barr virus, or influenza. Such post-viral conditions over the last 100 years have been given a plethora of different names but from about 2016 the common name of Myalgic Encephalomyelitis / Chronic Fatigue Syndrome (ME/CFS) has settled to encompass them all. Derived from two isolated infectious disease outbreaks, first in London (ME) [6] and second in Incline Village, Nevada (CFS) [7], it has been accepted as documenting the same illness.

LC has arisen from the huge case numbers of COVID-19 from the single triggering virus, SARS-CoV-2 and that has meant a sudden huge case burden of LC, as distinct from the slow build-up of cases of ME/CFS from the multiple triggers, boutique outbreaks, endemic viruses or other major stressors. Since experience has shown the large majority of patients diagnosed with ME/CFS have the condition as a lifelong illness, the absolute numbers of worldwide cases slowly increase with each new case [8]. The LC onset scenario awakened the clinical and scientific communities to the severely debilitating nature of these diseases. It has highlighted the lack of prior investment in research into understanding the ME/CFS post-viral/stressor syndrome. ME/CFS patients have been coined the 'missing millions' in protest that the impact of their condition on their lives has been met with inadequate recognition and support from clinical and social services [9]. The hope is that the current focus and large research investment in LC will benefit both ME/CFS and LC patients in finding management solutions and treatments to improve their quality of life. A reversal of the debilitating symptoms with a new understanding of these conditions might be possible, given the evidence that the neurological dysfunctions are not neurodegenerative.

For the 5 -10% of the population who have genetic or co-morbidity susceptibility to develop LC and ME/CFS [2,10], new COVID infections will continue to generate these debilitating ongoing post-viral conditions at a significant frequency. Recent data from Fang et al [11] showed rates of LC were similar in unvaccinated (8.4%) and people vaccinated with two doses (8.7%) but reduced in those who had had a third vaccination booster (5.8%). A study that examined the records of >400, 000 US veterans who had the infection during the period March 2020 to February 2022 at one year post infection in the unvaccinated group the rates declined from 9.5 % (delta variant) to 7.7% (omicron variant), and in the vaccinated the rates were 5.3% (delta) and 3.5% (omicron) [12]. Nevertheless, even with these lowered rates newly COVID-infected people are still developing LC, with the virus now becoming endemic, adding constantly to the global health burden.

Strong linkage of genetic factors to the susceptible group who develop the post-viral/stressor conditions has recently been discovered, after Precision Life (Oxford) added a combinatorial platform to GWAS technology that allowed combinations of single-nucleotide polymorphisms (SNPs) to be evaluated. It showed small clusters of SNPs in combination are linked to ME/CFS [13] and LC [14]. For example, in the ME/CFS study 199 SNPs in 15 clusters of 84 communities each with 3-5 specific variations were linked to 14 genes, relevant to cellular mechanisms dysfunctional in ME/CFS. These genetic variations could account for 91% of the samples from ME/CFS patients in the United Kingdom Biobank. Long COVID with a more diverse cohort gave more complex results – with 73 genes linked to the condition but 39 of the SNPs detected were also linked to nine of the genes identified in the ME/CFS study [14].

A key question is whether what is known about ME/CFS provides a suitable model for insight to understanding the ME/CFS-like syndrome subgroup of LC that represents ~50% of the cases [15,16]. Conversely, will new research findings emerging from studies of LC like the NIH's RECOVER initiative [17] benefit ME/CFS patients? Underpinning these questions is whether the physiological responses in susceptible people to the SARS-CoV-2 virus are similar or significantly different from those responses in ME/CFS patients who have had a diverse range of stress triggers leading to their ME/CFS. The current study aims to provide evidence on this question.

There is a wide array of >200 symptoms reported by both groups of LC and ME/CFS patients, of which >95% overlap suggesting high similarity at least in the clinical phenotypic effects on the patients [18,19]. Indeed several authors have referred to LC as being appropriately renamed ME/CFS if it lasts beyond two years, for example [3]. LC has been with us for only five years and it might present biologically in research studies currently as a juvenile form of ME/CFS, since the mean time

of those affected with ME/CFS and being studied is generally from onset up to ten years and beyond. However, a wide range of biological dysfunctions is already known to be common to the two conditions [10]. In 2022 Komaroff listed many: dysautonomia, generation of autoantibodies, switch in energy generation, low energy/hypometabolic state, increased oxidative stress, mast cell activation, abnormal cardiopulmonary responses to exercise tests, blood vessel/coagulation disturbances, Epstein Barr virus and other herpes viral reactions, small fibre neuropathy, cognitive dysfunction, disturbed HPA axis, neuroinflammation, and gut microbiome changes [20]. Importantly, those LC patients affected with the ME/CFS-like syndrome experience the same core defining symptom of ME/CFS, post-exertional malaise, but with some differences in its expression that were attributed to the early stage of the condition in LC [21].

Our recent comparative study of immune cell protein dysregulation in LC and ME/CFS identified a group of differentially regulated proteins common to both ME/CFS and LC patients. In most cases the proteins were up- or down-regulated similarly but in a minority of cases the differential regulation occurred in opposite directions. Similar molecular pathways were affected, for example, mitochondrial functions linked to energy production, immune system processes and cytokine regulation. Major overlapping clusters in both cohorts were found among proteins related to gene expression. An overarching conclusion from this study was that LC and ME/CFS have similar major dysfunctions in their immune cell physiology and energy production [22].

A recent comparative investigation of both adaptive and innate immune dysregulation underlying ME/CFS and long COVID highlighted the potential importance of immune exhaustion in disease progression. Differential gene expression analysis in ME/CFS showed downregulated IFN signaling and immunoglobulin gene expression, indicative of immune suppression, and pathway analysis implicated dysregulated macrophage activation, cytokine production, and immunodeficiency signaling. Long COVID patients had antigen presentation, cytokine signaling, and immune activation dysregulated with differentially expressed genes also associated with B cell development, macrophage activation, and cytokine signaling [23].

Comparative genome-wide DNA methylation studies in ME/CFS and LC have not yet been carried out, but there are studies on ME/CFS patients utilizing mononuclear immune cells or specific immune cell subtypes and using either Reduced Representation Bisulfite Sequencing (RRBS) [24,25], or Illumina Methylation 450K/EPIC arrays [26–30]. Our first RRBS-based analysis of ME/CFS patients identified 76 differentially methylated fragments and 394 differentially methylated cytosines linked to 122 genes involved in neurological, immune, and metabolic pathways [24]. A ME/CFS relapse-recovery longitudinal study we conducted on two ME/CFS patients and a matched control identified 577 differentially methylated fragments during the relapse with significant involvement in IL-8 signaling, NF κ B dysregulation, and neutrophil degranulation. The methylation changes at individual sites reverted to the levels prior to the relapse when the relapse resolved [25].

In this current comparative study of LC and ME/CFS we have examined the DNA methylome landscape of age/sex linked LC and ME/CFS patient cohorts and healthy controls.

2. Results

2.1. Whole-Genome DNA Methylation Patterns:

Genome-scale DNA methylation changes were derived from the samples from each of five Healthy Controls (HC), five ME/CFS patients, and five LC patients. There were 342,055 fragments that covered 2,151,222 CpG sites in the 15 samples, from a total of 3.1×10^8 sequence reads (9.2×10^7 for HC, 10.8×10^7 for ME/CFS, and 10.9×10^7 for LC) allowing for comprehensive genome-wide analysis (Table S1). The global methylation genomic patterns were assessed and the median value obtained for global methylation with all three cohorts was similar (median methylation = 89.3% for HC, 89.9% for ME/CFS, and 88.7% for LC) showing hypermethylation was predominant. The promoter regions were, by contrast, predominantly hypomethylated in all three cohorts (Table S2). The intronic and exonic regions were predominantly hypermethylated with a similar median in all cohorts and with

a slight increase in the first quartile in the ME/CFS cohort. A flow diagram of the decisions for analysis of the DMFs between ME/CFS and LC is shown in Figure 1.

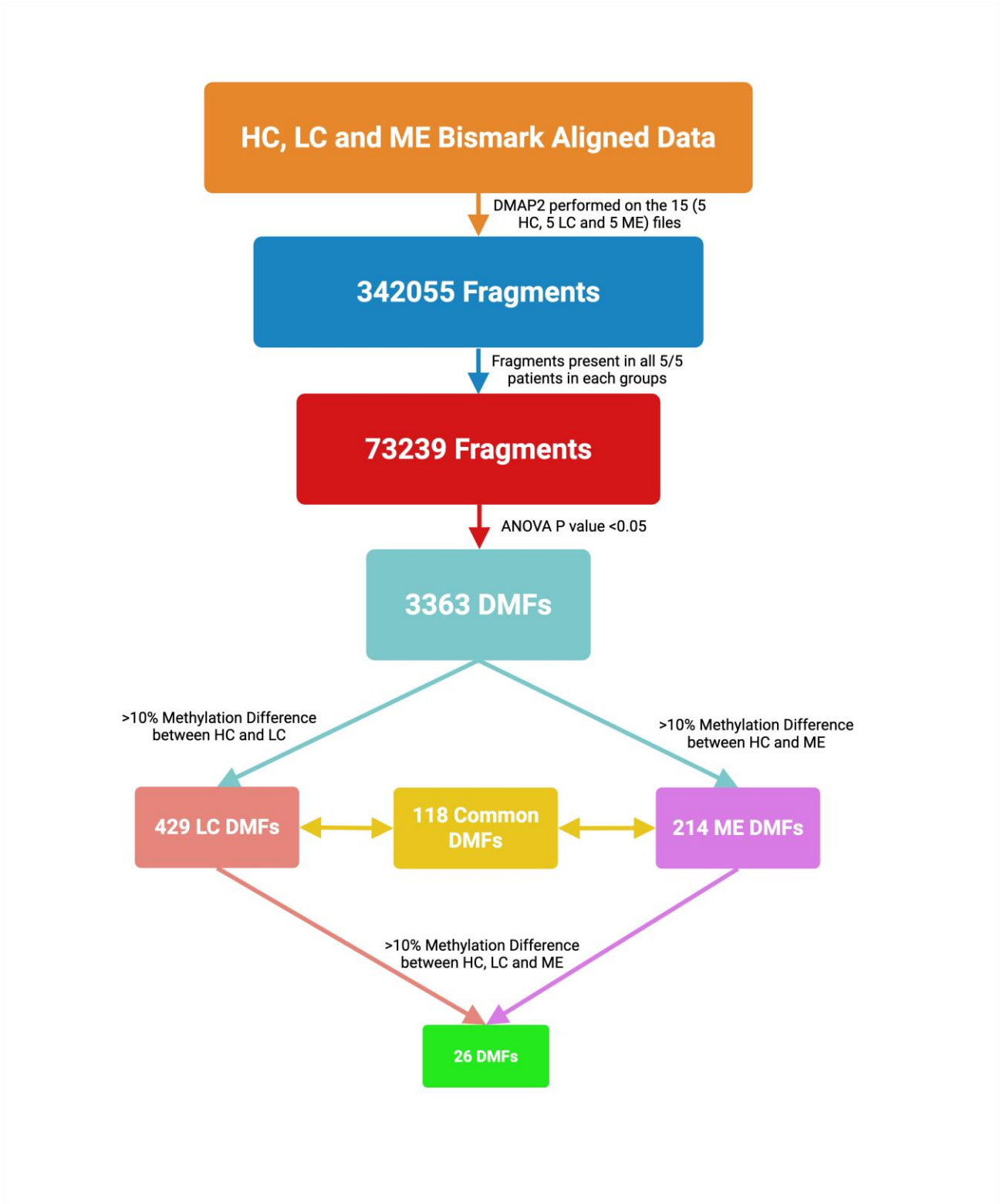


Figure 1. Flow diagram of the analysis of the DMFs in the ME/CFS, LC cohorts compared with age/sex matched HCs. Bam files were created from the Reduced Representation Bisulphite Sequencing (RRBS) data, the 15 samples analysed by DMAP2 [31] to give 342055 methylated fragments, those fragments found in all five patients of each of the three cohorts made were sub-selected (73239 fragments), and those significantly different ($p < 0.05$) comparing the ME/CFS and LC cohorts with HCs identified (3663 DMFs). Applying a limit of 10% change in differential methylation from the HCs gave 429 LC DMFs and 214 ME/CFS DMFs of which 118 were in common

between the two disease cohorts. Twenty-six of these 118 had a >10 % methylation difference between the two patient cohorts.

To begin the evaluation of the methylation landscape, the fragments were first sub-selected with a strict criterion as being present in all five patients of each of the three cohorts, and 73,239 fragments were then available for further analysis (Figure 1). A Principal Component Analysis (PCA) separated the cohorts into three distinct clusters (Figure 2). This indicated that both the ME/CFS and LC cohorts showed differential methylation within these common fragments compared with the healthy controls. The separation of the ME/CFS and LC cohorts into individual clusters (Figure 2) suggested that there might be differences between the extent of the methylation change at specific sites between the two cohorts, or changes at specific sites in only one of the disease cohorts. For this analysis a significance of $P < 0.05$ was imposed for the methylation change, but no limits on the degree of methylation change. For this analysis, 3363 fragments met that criterion.

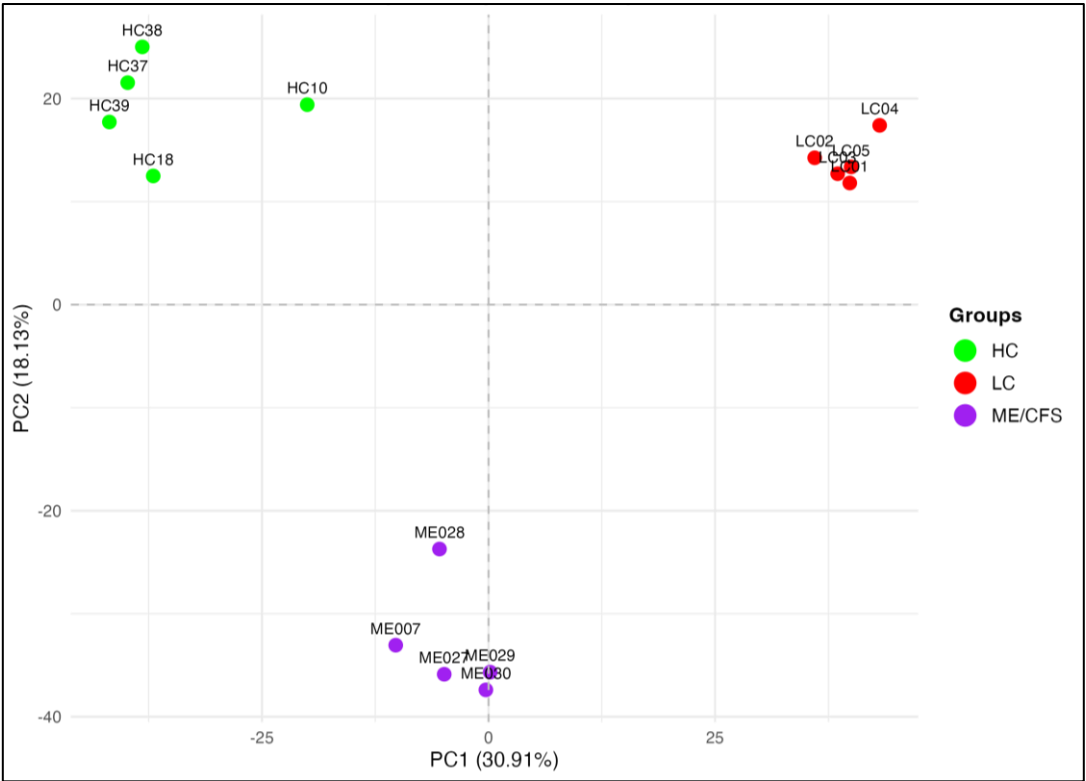


Figure 2. PCA of differentially methylated fragments in all members of the HC, LC, ME/CFS cohorts. PCA plot illustrating three distinct clusters representing HC, ME/CFS, and LC based on 3,363 DMFs common to all cohorts filtered by $P < 0.05$, without considering methylation difference.

2.2. Characteristics of the Differential Methylation Changes in LC and ME/CFS

The analysis identified 429 DMFs between LC vs HC (Table S3, Figure 1) and 214 DMFs between ME/CFS vs HC (Table S4, Figure 1) (p -value < 0.05 , minimum 10% methylation difference). Of the 429 DMFs between LC and HC, 148 were hypomethylated and 281 were hypermethylated, and among the 214 DMFs between ME/CFS and HC, 69 were hypomethylated and 145 were hypermethylated. Thus, both cohorts showed methylation patterns shifting towards hypermethylation when compared to HCs and in this study, LC patients show more abundant methylation changes than the age/sex matched ME/CFS patients. Of the 429 DMFs in LC and 214 DMFs in ME/CFS when compared to HC, 118 DMFs were common to both disease datasets, as shown in the Venn diagram (Figure 3A). The Pearson R score was 0.88 when the methylation data within the common fragments of the two cohorts were compared, indicating a high correlation between the data at the differentially methylated sites from the LC and ME/CFS cohorts and emphasizing the similarity between the two conditions. Heat

maps of LC vs HC and ME/CFS vs HC are shown in Figure 3B,C. Unsupervised hierarchical clustering of DMFs between HCs and LCs (Figure 3B) and between HCs and ME/CFS (Figure 3C) has separated the differential methylation patterns so that all members of each of the three cohorts (HC-green, LC-red, or ME/CFS -purple) group together. The regions of the genome from which the DMFs are derived (intergenic, promoter, exon, intron or the boundary between intron and exon) are shown on the axis at left, colour coded in the key. The heatmaps showed distinct patterns of the DMFs: (i) most hypermethylated fragments in the HC cohort became more strongly hypermethylated in both LC and ME/CFS cohorts, and a minority became more hypomethylated; (ii) most hypomethylated fragments in the HC generally also became more hypermethylated but with a minority becoming more hypomethylated. This was a common pattern for both disease cohorts. The minority group of DMFs was larger in the LC cohort than in the ME/CFS cohort (iii) Some fragments with mid-range methylation were more variable in their methylation among the individual members of the HC cohort but became predominantly more hypermethylated in the patient cohorts, again with a minority showing greater hypomethylation. A heatmap illustrating the methylation values and genomic location of the 118 common fragments (Table S6) found in each cohort compared with the HC cohort was generated and showed the majority of these DMFs are similarly differentially methylated (Figure 3D). In contrast to the heat maps in Figures 3B,C, unsupervised hierarchical clustering of DMFs has separated one ME/CFS patient (ME028) in the ME/CFS group from the other ME/CFS members into a 'group of one' whereas all five members of each of the other two cohorts (HC-green, LC-red) group together. It is interesting to note that in the PCA analysis shown in Figure 2 this patient ME028 was more widely separated from the other members of the ME/CFS cluster. The heat map showed a wide range of methylation levels in the HC of the 118 fragments and both changes towards hypermethylation and hypomethylation in the LC and ME/CFS cohorts.

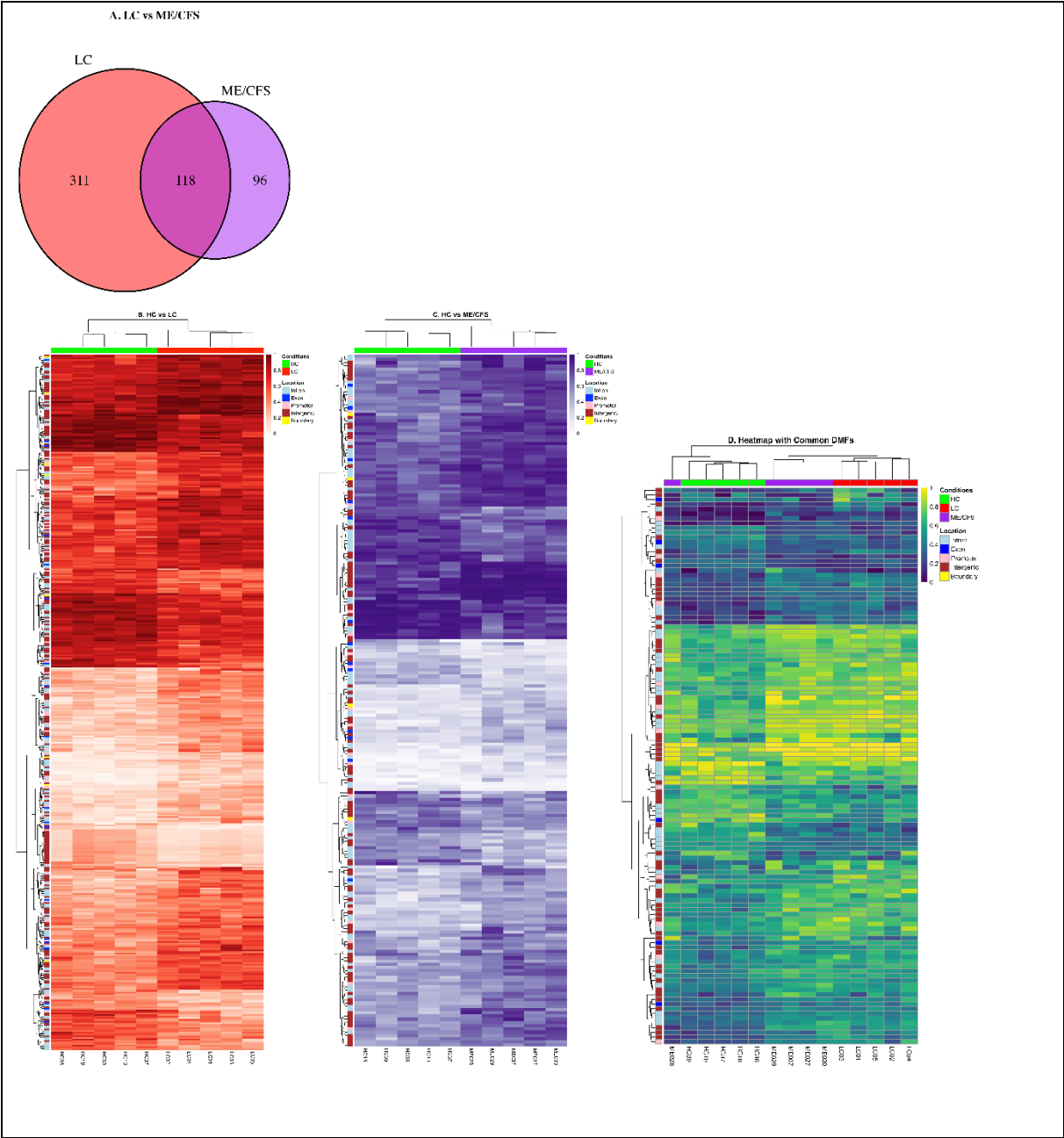


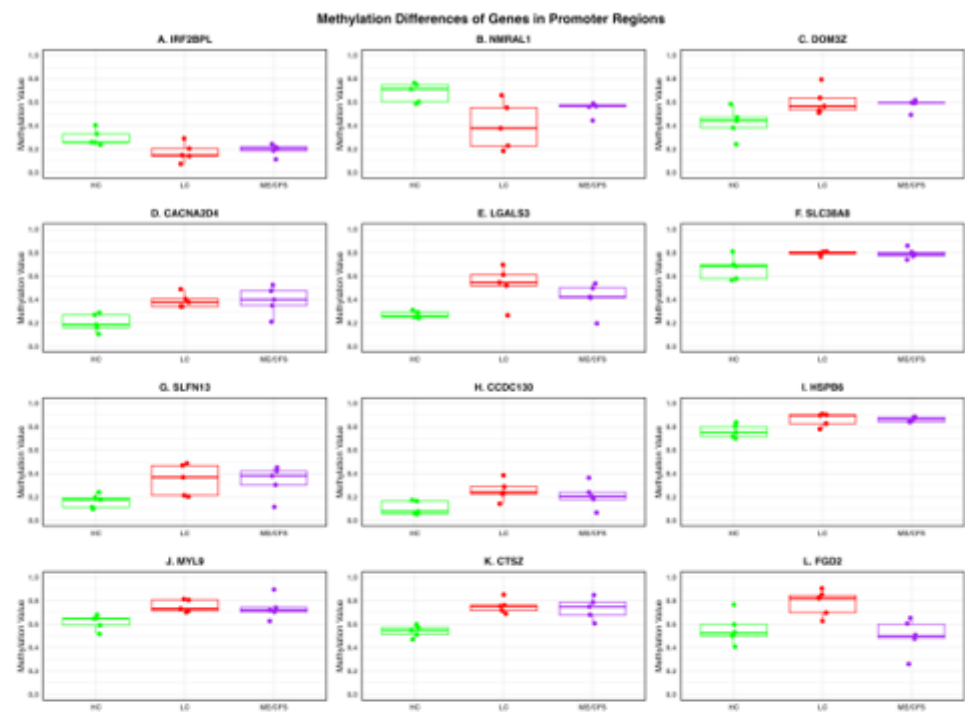
Figure 3. Heatmaps of differential methylation on fragments in LC and ME/CFS patient cohorts compared with HCs. (A)Venn diagram showing overlapping DMFs in LC and ME ($P<0.05$, $>10\%$ methylation difference). Heatmaps show DMFs between (B) LC and HC, (C) ME/CFS and HC ($P<0.05$, $>10\%$ methylation difference). The annotation column bar at the top of each heat map represents the cohort group (LC-red, HC-green, ME/CFS - purple), and the annotation on the Y axis shows the genome region of the DMF (color coded in the key). The colour gradient shown in the key indicates the methylation level of the fragments with the darker colours representing the higher degree of methylation. The locations of the DMFs are annotated beside the heatmaps, gene promoters (-1kb to +5kb from the TSS), exons, introns, and intergenic elements (>5 kb upstream from the nearest TSS), and intron-exon boundary elements. (D) Heatmap showing the methylation values of the 118 common DMFs in the ME/CFS and LC cohorts and illustrating the methylation differences in LC and ME/CFS patient groups compared with the HC group. The annotation column bar at the top of the heat map represents the cohort groups (LC-red, HC-green, ME/CFS-purple), and the annotation row bar on the left side shows the genome region of the DMFs (colour coded in the key). The colour gradient yellow to indigo shown in the key ranges from hypermethylation (yellow) to hypomethylation (indigo). It indicates the colours matching specific methylation values.

2.3. DMFs Associated with Gene Promoters and Gene Exons.

Among the 118 common DMFs, twelve were associated with *gene promoters*. Nine (associated genes-*LGALS3*, *SLC38A8*, *SLFN13*, *CCDC130*, *HSPB6*, *CTSZ*, *MYL9*, *DOM3Z*, *CACNA2D4*) showed hypermethylation in both LC and ME/CFS, and two (associated genes -*IRF2BPL*, *NMRAL1*) were hypomethylated in both conditions. In contrast, one, associated with *FGD2* was hypermethylated in the LC patients and hypermethylated in the ME/CFS patients when compared with healthy controls. Six fragments were associated with *gene exons* (*ITPKB*, *KIF26B*, *CHD7*, *STAT5A*, *ABCA7*, *HSPA12B*) among the 118 common DMFs. Three (*ITPKB*, *KIF26B*, *CHD7*) were hypomethylated in both the LC and ME patients, and two (*STAT5A*, *ABCA7*) were hypermethylated in both conditions. By contrast, one *HSPA12B* showed hypermethylation in LC and hypomethylation in ME/CFS compared to HC (Table S5). The twelve identified DMFs in promoter regions associated with specific genes are shown as box plots in Figure 4A, indicating the individual values of the five patients from each disease cohort and the controls. In most cases the changes were found in all patients of the cohort and variation among the individual patients was relatively small, apart from two sites for the LC cohort. The HC median values of the two promoter sites that were hypomethylated in both cohorts (*IRF2BPL* and *NMRAL1*) were significantly different, 25% and 75% methylation respectively. For the eight sites that were hypermethylated in both LC and ME/CFS compared with HCs, the median values of the methylation in the HCs varied from 9-75%. The promoter site associated with *FGD2* that was hypermethylated only in the LC patients compared with the HC increased from 52% to 81% whereas it was unchanged at 50% in the ME/CFS cohort.

The box plots of the six DMFs associated with exons of specific genes, *ITPKB*, *KIF26B*, *CHD7*, *STAT5A*, *ABCA7*, and *HSPA12B* are shown in Figure 4B. Most had HC methylation median values of ~40%. The variations in the methylation values among individual patients, while greater than in the controls, were still relatively small.

A. DMFs associated with gene promoters



B. DMFs associated with gene exons

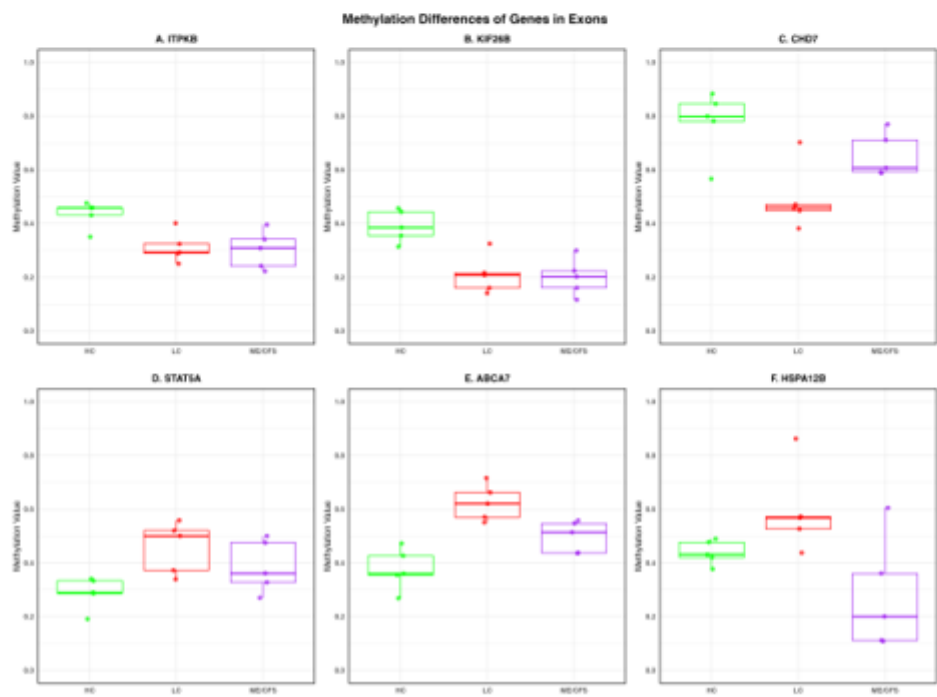


Figure 4. Box plots showing individual patient differential methylation characteristics at gene-associated sites. Box plots of (A) the twelve genes associated with differentially methylated promoters and (B) six genes associated with differentially methylated exons (B) identified within the 118 fragments in common between LC and ME/CFS patients. The plots show the individual patient values of the LC, ME/CFS and the HC cohorts. In both A & B, the HC are coloured green, the LC red and ME/CFS purple. Individual patients are indicated by the points on the plots. The medians are indicated by the bold line and the box indicates the first and third quartiles. Associated gene IDs are displayed at the top of each plot.

2.4. Methylation Differences Between Long COVID and ME/CFS

There were also differences in the *degree* of methylation change between the two disease cohorts. There were 26 DMFs among the 118 DMFs with >10% methylation difference between LC and ME/CFS (Table S6). Fifteen of the 26 DMFs lie within the intergenic regions and 11 are in more defined gene regions and therefore easier to interpret. Of these 11 DMFs, three of the genes corresponding to sites within exons (*CHF7*, *ABCA7* and *HSPA12B*) and three within promoter regions (associated with *FGD2*, *NMRAL1*, *LGALS3*).

In Table 1 the chromosome and the genomic start and end sites of the 26 DMFs where there was a >10% difference in the methylation changes between LC and ME/CFS cohorts are shown. The genomic locations of the DMFs (promoter, exon, intron or intergenic) are documented and the percentage differences in methylation between LC vs HC, ME/CFS vs HC and then LC vs ME/CFS indicated. GeneIDs linked to differentially methylated promoters, exons, and introns are given but not the possible gene linkages for intergenic regions. The DMF changes between the two cohorts are sorted according to the degree of difference between the LC and ME/CFS (-29% to + 37% - shown in last column). It is to be noted that the exons and promoters in Table 1 are already represented in the box plots in Figure 4A,B.

Table 1. Twenty-six DMFs segregating HC, LC and ME/CFS cohorts from each other.

Chr	Start	End	Location	GeneID	%Difference LC v HC	%Difference ME v HC	%Difference LC v ME
18	34854648	34854693	intron	<i>CELF4</i>	-13.9	+15.1	-29.0
1	90074598	90074699	Intergenic		-36.4	-15.7	-20.7
16	4527540	4527641	Promoter	<i>NMRAL1</i>	-32.0	-12.5	-19.5
5	39185995	39186145	intron	<i>FYB</i>	-33.3	-14.5	-18.8
2	240241154	240241261	Intergenic		+13.4	+32.2	-18.8
7	158766236	158766379	Intergenic		+18.4	+35.4	-17.0
8	61778005	61778136	exon	<i>CHD7</i>	-29.2	-14.5	-14.7
17	76129099	76129221	intron	<i>TMC8</i>	-24.7	-13.3	-11.4
6	30854000	30854160	intron	<i>DDR1</i>	-22.4	-11.0	-11.4
17	75429645	75429795	Intergenic		-21.9	-10.6	-11.3
1	59090260	59090360	Intergenic		+12.4	+22.8	-10.6
2	121955379	121955533	Intergenic		+22.3	+12.2	+10.1
16	3137553	3137716	Intergenic	<i>ZNF205</i>	+26.1	+14.7	+11.4
19	1047184	1047347	exon	<i>ABCA7</i>	+24.6	+11.8	+12.8
7	158250978	158251159	Intergenic		+28.1	+15.3	+12.8
14	55587537	55587752	Promoter	<i>LGALS3</i>	+28.5	+14.8	+13.7
15	75336231	75336352	intron	<i>PPCDC</i>	+26.5	+10.8	+15.7
8	58055165	58055309	Intergenic		+27.6	+11.7	+15.9
21	46714776	46714890	Intergenic		+31.5	+13.8	+17.7
8	58055310	58055463	Intergenic		+34.2	+15.7	+18.5
1	19110747	19110909	Intergenic		-16.7	-35.4	+18.7
17	76661321	76661487	Intergenic		+11.8	-11.3	+23.1
10	118025165	118025303	Intergenic		+13.1	-13.1	+26.2
6	36969405	36969621	Promoter	<i>FGD2</i>	+21.7	-11.1	+32.8
20	3732943	3733092	exon	<i>HSPA12B</i>	+18.3	-15.6	+33.9
3	126945870	126946029	Intergenic		+11.4	-25.9	+37.3

Chr is the chromosome number where the DMF is found, the start and end sites of the DMF in the genome are shown, the location of genomic region indicated, GENEID -deduced associated gene, % methylation differences between LC v HC (first column), ME/CFS v HC (second column), LC v ME/CFS (third column). - hypomethylation, + hypermethylation % difference.

In the eight of the 26 DMFs where there was hypomethylation in both cohorts, it was greater in seven in the LC patient group, and in only one fragment in the ME/CFS patient group. In the 12 of the 26 DMFs that were hypermethylated in both cohorts, nine showed greater differential methylation in the LC cohort and three in the ME/CFS cohort. Hence, the LC group of patients generally have a greater change in their methylation status in 16 of the 20 DMFs compared with the ME/CFS patients when the change is in the same direction. By contrast, six of the 26 DMFs showed opposite changes in their differential methylation in the two cohorts (five hypermethylated in LC but hypomethylated in ME/CFS; one hypermethylated in ME/CFS and hypomethylated in LC).

2.4. Functional Pathway Analysis of the DMFs of Long COVID and ME/CFS

Among the 429 DMFs from HC vs LC and 214 DMFs between HC vs ME, the unique associated GeneIDs were isolated and tabulated, except from sites within the intergenic regions where gene linkages are much less certain. There were 215 unique genes linked to LC (Table S8) and 111 genes linked to ME/CFS (Table S9). To identify the functional pathways associated with the DMFs in LC and ME/CFS, pathway enrichment analysis was performed using Metascape [32]. This analysis revealed several shared pathways between the two conditions (Figure S1A & S1B), suggesting common biological mechanisms. Notably, **Response to Wounding (GO:0009611)** emerged as a key pathway involved in tissue repair and inflammatory processes, aligning with the immune dysregulation and chronic inflammatory responses observed in both conditions. Additionally, **Regulation of System Process (GO:0044057)** was significantly enriched, highlighting disruptions in physiological processes such as circulation and metabolism that may contribute to cardiovascular and neurological dysfunctions. **Cellular Response to Cytokine Stimulus/Acid Chemical (GO:0071345/GO:0071229)** was identified, which likely reflects the important role in immune signaling and inflammation, both of which are known to be altered in ME/CFS and LC. Furthermore, **Regulation of Small GTPase-Mediated Signal Transduction (GO:0051057/GO:0051056)** was enriched, implicating intracellular signaling pathways that modulate immune responses, cell migration, and tissue repair. **Growth Regulation (GO:0040007/GO:0040008)** was a prominent pathway, suggesting that aberrant growth signaling could contribute to impaired tissue regeneration in both conditions. Other than these similarities, the functional pathway analysis showed blood vessel morphogenesis, muscle organ development, AGE RAGE pathway, Neutrophil degranulation as other notable pathways in LC, whereas thyroid hormone production, leukocyte differentiation, negative regulation of T cell receptor pathway, heart development and blood circulation were highlighted in ME/CFS.

3. Discussion

Although a preliminary patient study, the findings described here provide deep insights into the genome-wide DNA methylation landscape of LC and ME/CFS, consistent among the patients in each cohort, and highlight both important similarities as well as differences between these conditions. The latter may reflect simply the differences in the time from onset of each condition in the patients, with the LC group at one year still in the acute stage as a 'juvenile' form of the more well-established ME/CFS, here represented by chronic stage patients. A proportion of the differences in LC may reflect the specific characteristics of the viral trigger associated with the SARS-CoV-2 virus. This virus likely invokes unique molecular responses as well as similar responses to the other ME/CFS-causing stressors within the broad categories of the dysfunctional physiology but still supporting a very similar clinical phenotype. This can be explored in future studies matched not only by age and sex but also by time of onset.

Principal Component Analysis (PCA) of differentially methylated fragments identified in all patients of the three cohorts showed distinct clustering of the HC, LC, and ME/CFS cohorts, demonstrating that, despite LC and ME/CFS having many changes in methylation at genomic sites in common, the global DNA methylation patterns can separate the two disease groups from each other as well, and both are well separated from the HC group. However, the extent of differential

methylation was generally more pronounced in LC than in ME/CFS, with LC patients showing a greater number of differentially methylated fragments (DMFs) when compared to HCs. This can explain why the ME/CFS and LC cohorts cluster separately. The maximum length of time possible for LC cohorts since the start of the pandemic have had their condition is now 5-6 years compared with ME/CFS cohorts of 40-50 years or even more, and so future studies with these ME/CFS-like conditions through the disease stages will help to understand these apparent differences better. For example, the epigenetic DNA methylations changes may be more dynamic at earlier stages, whereas at later stages, as with the age/sex matched ME/CFS cohort in this study, there may be a lowered expression of the initial changes leading to the chronic debilitation in patients that has become more stable with time.

The hierarchical clustering of the methylation changes in the 118 DMFs shared between LC and ME/CFS demonstrated a high degree of correlation (Pearson R = 0.88), indicating substantial overlap between the two conditions. Interestingly, in the PCA reflecting the global methylation patterns of 3363 DMFs p<0.05 present in all patients of the three cohorts (Figure 2) one ME/CFS patient, ME028, while still within the cluster, was more separated from the other patients. This patient also separated from the other ME/CFS patients in the unsupervised clustering shown in the heat map of Figure 4D. It is the youngest patient in the cohort and the onset to study time was much lower than the others in the ME/CFS cohort. It is well documented that the DNA methylome can change with age among all cultural groups [33]. In this study we had one example of an older age/sex matched ME/CFS and LC patients and HC compared with the other 4 patients of each cohort (see Table 4-Methods). Interestingly, the older healthy control, HC10 in the PCA of Figure 2 is separated from the other HCs. However, in contrast the two matched older ME/CFS and LC patients are tightly clustered within the other patients of their cohorts, suggesting the changes in the DNA methylome caused by the disease are more influential than those reflecting age.

The shared 118 DMFs in the ME/CFS and LC patients were primarily linked broadly to immune regulation and metabolic pathways, further supporting the hypothesis that LC and ME/CFS share common biological mechanisms. Table 2 shows the characteristics of the 15 DMFs that could be confidently linked to specific genes (i.e. in eight promoters and seven gene bodies) that were shown in Box plots with individual patients’ values in Figure 4A & B. Those in intergenic regions were not included here as connections to specific genes could be only tentatively inferred.

Table 2. Differentially methylated fragments at promoters and exons common to both ME/CFS and LC patients.

A. Promoters						
Chromosome	Start	End	Associated Genes	DM*(%) (LC vs HC)	DM*(%) (HC vs ME)	DM* (%) (LC vs ME)
19	13841885	13841989	CCDC130	+14.2	+11.8	+2.4
14	77495636	77495807	IRF2BPL	-12.2	-10.2	-2.0
17	33776642	33776791	SLFN13	+18.1	+11.7	+6.4
16	84076941	84077080	SLC38A8	+12.7	+13.0	-0.3
19	36249868	36250044	HSPB6	+11.1	+10.3	+0.8
16	4527540	4527641	NMRAL1	-32.0	-12.5	-19.5
14	55587537	55587752	LGALS3	+28.5	+14.8	+13.7
20	57581333	57581441	CTS2	+21.2	+18.2	+2.8
20	35170171	35170286	MYL9	+13.2	+11.6	+1.6
12	2027243	2027352	CACNA2D4	+17.7	+17.6	+0.1
6	36969405	36969621	FGD2	+21.7	-11.1	+32.8
6	31939186	31939321	DOM3Z	+21.4	+15.6	+5.8
B. Exons						
1	245851466	245851609	KIF26B	-19.0	-18.7	-0.3
8	61778005	61778136	CHD7	-29.2	-14.5	-14.7

1	226821736	226821914	<i>ITPKB</i>	-12.1	-13.1	+1.0
17	40463432	40463555	<i>STAT5A</i>	+16.2	+11.4	+4.8
20	3732943	3733092	<i>HSPA12B</i>	+18.3	-15.6	+33.9
19	1047184	1047347	<i>ABCA7</i>	+24.6	+11.8	+12.8

‘Start and end’ refer to the genomic numbering of the start and end of the DFM. *DM (%) is the percentage differential methylation.

At nine of the twelve promoters the degree of change was similar for the ME/CFS and LC patients, whereas in the other three promoters there was a much greater change in the methylation of the LC patients. Nine promoters exhibited hypermethylation, whereas two were further hypomethylated. In one promoter the changes were in opposite directions, hypermethylation for the LC patients and hypomethylation for the ME/CFS patients. For the six common DMFs in gene exons, five had similar degrees of change in both ME/CFS and LC patients, with three showing much greater changes in the LC patients, and one of those sites was more hypermethylated in LC but conversely more hypomethylated in ME/CFS.

Among the genes that were linked to the specific twelve gene promoters (Table 2A), the gene product of the intron-less gene *IRF2BPL* is deduced to be an interferon regulatory factor 2 binding protein involved in central nervous system function [34] NMRAL1 is a redox-sensitive protein that also negatively regulates the activity of NF-kB, implicated in regulating the immune response and inflammation [35]. LGALS3 is also involved in inflammation and innate immunity, important for macrophage adhesion and T cell regulation [36]. *SLC38A8* is a gene responsible for a Na⁺ coupled neutral amino acid transporter with a preference for the neurotransmitter glutamate [37]. *SLFN13* is a gene whose gene product is an RNASE engaged in translational control and can inhibit a wide range of viruses [38]. CCDC130 protein is a likely mRNA splicing factor with an integral part in the function of spliceosome [39]. HSPB6 is a heat shock protein, with a role in platelet function which is likely to play a role in human muscle function [40], and CTSZ is a cathepsin in the family of cysteine proteases, reported to be protective in inflammatory gastric disease [41]. *MYL9* encodes a myosin regulatory light chain that may regulate muscle contraction [42], and *CACNA2D4* is a voltage-gated calcium channel alpha(2)delta-4 subunit [43]. FGD2 is expressed in B lymphocytes, macrophages and dendritic cells and affects antigen uptake, antigen presentation and cell migration [44]. DOM3Z gene product has a role in pre-mRNA quality control and has been connected with the autoimmune disease, Systemic Lupus Erythematosus [45] Thus, the differential methylation of the twelve gene promoters affects genes that have functions that are related directly or indirectly related to immune functions, a key feature of the pathophysiology of the LC and ME/CFS conditions.

In case of the six differentially methylated exons (Table 2B), the specific genes have more specific diverse functions. The gene product *ITPKB* is involved in signal transduction with calcium release in the endoplasmic reticulum related to cytokine production in T cells [46], and the *KIF26B* protein is intracellular motor protein transporting organelles along microtubules [47]. *CHD7* encodes a helicase DNA-binding protein involved in transcriptional regulation [48], while the *STAT5A* is a gene product that is critical for signal transduction and activation of transcription, mediating cellular responses to cytokines for proliferation, differentiation and apoptosis [49]. *ABCA7* protein is an ATP-binding cassette (ABC) lipid transporter linked to an increased risk of Alzheimer’s disease [50,51]. The *HSPA12B* gene is an atypical heat shock gene thought to be essential for angiogenesis and cell migration [52]. These findings suggest that changes to the expression of specific regulatory factors, identified as related to the immune system in some cases, may act as drivers of the distinct disease phenotypes of both LC and ME/CFS.

Genes associated with the ME/CFS DMFs of this study (HC vs ME) were compared with that of our previous study of Helliwell et al., 2020 [23], where DMFs were identified between HC and ME (>15% mean methylation difference). The comparison identified genes in common mostly linked from introns, but the methylation changes were in fragments at different sites within the introns in the two studies. The actual functions of differentially methylated sites in introns are not clarified yet, or

whether an individual gene can be influenced by different sites within one of its introns that can be many kilobases in length. However, it is compelling that the functional categories of the genes, shown in the last column of Table S9 can be linked to the dysfunctional physiology in ME/CFS and LC, for example, transcription factors, signal transduction, calcium channels, and mitochondria. Four of the six were similarly hyper- or hypomethylated in both studies whereas in two cases the DMF affected the methylation in opposite directions. The reason for the opposite direction could be explained by different DMFs in the intron being associated with the gene regulation. The five gene-associated genomic sites with highest differential methylation were introns in both studies. Additionally, one gene was linked to a fragment in an exon in our study, but to an intergenic site in the Helliwell et al (2020) study [23].

Functional pathway analysis (Figure S1A & S1B) using Metascape [32] revealed key shared pathways between LC and ME/CFS, with significant enrichment in immune regulation, response to wounding, cytokine signaling, and small GTPase-mediated signal transduction. These pathways align with previous findings of immune dysregulation and inflammatory responses in both conditions. However, pathway enrichment also suggested condition-specific differences that may also relate to the triggering source for the condition (SARS-CoV-2 virus for LC, and other viral triggers for ME/CFS) or the stage of the disease condition. LC showed significant associations with blood vessel morphogenesis, neutrophil degranulation, and the AGE-RAGE pathway, while ME/CFS exhibited associations with thyroid hormone production, leukocyte differentiation, and T cell receptor regulation. These may reflect distinct differences in the immunopathological mechanisms underlying the stage of each condition, with the more juvenile LC (one year from onset in these patients) potentially involving more acute inflammatory and vascular responses, while the more mature ME/CFS (average 12 years in this age/sex matched cohort) may involve more chronic immune dysregulation mechanisms.

Using the same genes implicated in the generation of the data from Metascape, we explored their functions separately on Gene Cards and then utilised an AI tool to generate a broader functional category based on the functions derived from the Gene Cards. From this analysis a Sankey plot was produced to give a broader overview of the consequences of the differential methylation changes exhibited in each condition ME/CFS and LC. (Figure 6). The Sankey Plot gave four broad functional categories for both LC and ME/CFS: Transcription, Immune Function, Signal Transduction, and Cytoskeleton. LC was also associated with changes in lncRNA as a major category, whereas ME/CFS had an extra category of ion channels. These plots highlight that differential methylation for both Long COVID and ME/CFS affects similar major broad molecular physiological and biochemical pathways affirming the similar pathophysiology of the two conditions.

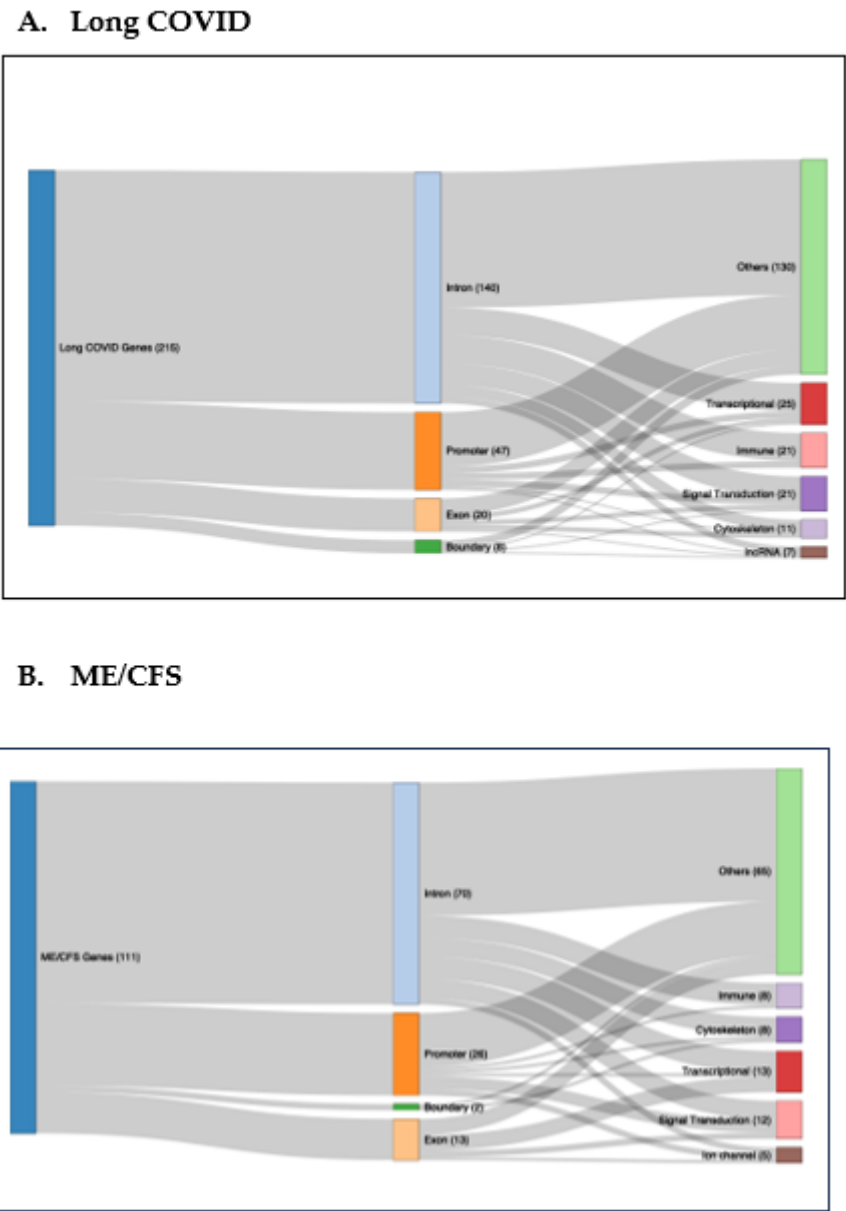


Figure 6. Sankey Plot showing the effects of differential methylation at regions of specific genes on molecular physiology of LC and ME/CFS. The figure demonstrates the connection of the differential methylation to gene regions of specific genes in A. Long COVID and B. ME/CFS. The locations of the sites within the genes (intron, exon, promoter, exon/intron boundary) and the main functional categories of molecular physiology affected, categorized by AI based on the functions derived from Gene Cards.

4. Materials and Methods

4.1. The Analysis Cohorts

We analyzed the DNA methylomes of five LC patients, five age/sex matched ME/CS patients, and five age/sex matched healthy controls (HC) by Reduced Representation Bisulphite Sequencing (RRBS) to identify differentially regulated DNA fragments in the three groups. The ME/CFS patients had been diagnosed using the Canadian Consensus Criteria (2003) by an expert ME/CFS clinician [53] and the LC patients from the combination of a positive test for COVID-19, and the subsequent development of symptoms indicating an ME/CFS-like syndrome [15], consistent with the WHO clinical case definition of 2021 [54]. The demographics of the three cohorts are shown in Table 3. Patients with ME/CFS and LC filled in detailed questionnaires seeking the origin and course of their

illness and the symptoms associated with it. The symptoms were graded on a severity scale of those symptoms. All were significantly affected (moderate to serious) but able to go to a community pathology laboratory to give their blood samples. No patient was classified as ‘severely ill’ that is, bedbound or completely housebound.

Table 3. Age/sex of the matched ME/CFS, LC, and HC cohorts.

Patient	Age	Sex	Patient	Age	Sex	Control	Age	Sex
ME030	40	F	LC01	43	F	HC18	46	F
ME028	19	F	LC02	27	F	HC39	26	F
ME027	65	F	LC03	65	F	HC10	59	F
ME029	40	M	LC04	42	M	HC37	40	M
ME007	27	F	LC05	36	F	HC38	31	F

4.2. PBMC Isolation

Patients completed a brief survey of their health status on the day at the time of blood collection. Blood fractions were processed within 24h. Peripheral blood mononuclear cells (PBMCs) were isolated from whole blood as described [55] by layering it onto Ficoll-Paque, followed by centrifuging at 400×g to separate plasma from PBMCs and the PBMCs from other cells. The removed PBMC layer was diluted with PBS and then pelleted at 100×g. The pellet was washed in PBS and stored at −80°C in a solution of FCS containing 10% DMSO.

4.3. DNA Extraction

DNA was extracted from 200 µL of the PBMC fraction using the Illustra Blood Genomic Prep Mini Spin Kit, following the manufacturer’s instructions. Elution was performed using the kit’s EB buffer, and DNA concentration was measured with a Qubit 2.0 fluorometer according to the Qubit dsDNA HS Assay Kit protocol.

4.4. Reduced Representation Bisulphite Sequencing

Reduced Representation Bisulphite Sequencing (RRBS) libraries were prepared following previously established protocols [56,57] In summary, 500 µg of genomic DNA was digested using 160 U of the MspI restriction enzyme. After end repair and adenylation of the 3’ ends, adaptors were ligated to the DNA fragments. Bisulfite conversion was carried out using the EZ DNA Methylation Kit (Zymo Research Corp, USA) according to the manufacturer’s instructions. A semi-quantitative PCR was performed on the bisulfite-converted DNA to determine the optimal number of amplification cycles required for the final large-scale PCR of the complete library. Following PCR amplification, DNA was size-selected using magnetic beads (AMPure XP beads from the TruSeq DNA nanokit -Beckman Coulter USA) as described in [51], isolating fragments between 40–220 bp to construct the RRBS libraries while minimizing adaptor contamination. The purified DNA was assessed for quality using a BioAnalyzer (Agilent, USA) and Qubit (Thermofisher Scientific, USA) measurements, followed by further purification with AMPure XP Beads (Beckman Coulter, USA).

4.4.1. DNA Sequencing

Samples were sequenced at the Otago Genomics and Bioinformatics Facility. After sequencing, raw FASTQ files were assessed for adaptor sequences and trimmed accordingly. The processed reads were then aligned to the human genome (GRCh37/hg19) using Bismark, generating BAM files for subsequent differential methylation analysis.

4.4.2. Statistical Analyses

Analyses were conducted using the updated version of the DMAP pipeline [58,59] namely the DMAP2 analysis pipeline [31] on a macOS computer to examine methylation changes across

fragments ranging from 40–220 bp. DMAP2 employed an ANOVA F-test to compare patient and control groups, ensuring that only fragments with data available for all individuals in each group were included. A raw p-value threshold of <0.05 was applied. We have used a stringent p-value threshold without false discovery rate correction in order not to lose true positives from this analysis, considering our sample size is low. Genomic features overlapping with these fragments were identified using the in-built Geneloc function of DMAP2. For the function of the genes, Gene Cards were used, and to assign the functional categories, Chatgpt was used using the functions from Gene Cards.

5. Conclusion

Globally the DNA methylomes of ME/CFS and LC patients were very similar to HCs. We have found differential methylation in the ME/CFS and LC cohorts associated with both promoters and gene exons that was mainly hypermethylation, with a minority of sites hypomethylated. There were examples of methylation changes in the opposite direction in the two cohorts. LC patients exhibited a greater number of changed methylation sites and at some of those in common with ME/CFS the extent of change in methylation was significantly greater compared with the ME/CFS patients. This contributed to the finding that the three cohorts LC, ME/CFS and HC each clustered separately in a Principal Component Analyses (PCA). A Sankey plot revealed the genes affected by the DNA methylation changes related to the same broad physiological/molecular functional categories in ME/CFS and LC: transcription, immune function, signal transduction, and cytoskeleton as those most significantly affected.

Supplementary Materials: The following supporting information can be downloaded at the website of this paper posted on Preprints.org. Table S1: Sequencing and mapping details of RRBS libraries (reference genome GRCh37). Table S2: Details of global methylation distribution in healthy, long COVID and ME/CFS 1. Table S3: Differentially Methylated Fragments ($P<0.05$, $>10\%$ methylation difference between HC and LC), related to Figure 3B. Table S4: Differentially Methylated Fragments ($P<0.05$, $>10\%$ methylation difference between HC and ME), related to Figure 3C. Table S5: Commonly Differentially Methylated Fragments ($P<0.05$, $>10\%$ methylation difference between HC and ME and $>10\%$ between HC and LC). Table S6: Differentially Methylated Fragments ($P<0.05$, $>10\%$ methylation difference between HC, LC and ME), related to Figure 5. Table S7: Associated Genes related to the DMFs in HC vs LC at promoters and gene bodies, related to Figure 6A. Table S8: Associated Genes related to the DMFs in HC vs ME, at promoters and gene bodies, related to Figure 6B. Table S9: Comparison of DMF-associated genes in the current study with Helliwell et al 2020 [23]. Figure S1A& S1B: Metascape Gene Enrichment Analysis for LC and ME/CFS genes associated with the DMFs excluding Intergenic sites.

Author Contributions: Conceptualization, W.P.T. and A.C.; methodology, A.C, E.J.R, P.A.S, K.P.; software, P.A.S.; validation, E.J.R.; formal analysis, K.P, S.S.; investigation, K.P, S.S, C.D.E.; resources, W.P.T, A.C., P.A.S.; data curation, E.J.R, S.S, K.P; writing—original draft /final preparation W.P.T.; writing—editing K.P, S.S, E.J.R, A.C; visualization, S.S.; supervision, W.P.T, A.C; project administration, W.P.T, K.P; funding acquisition, W.P.T, A.C. K.P and S.S have made equal contribution and are joint first authors. All authors have read and agreed to the published version of the manuscript.

Funding: The research was funded by Brain Research New Zealand CoRE (W.P.T), ANZMES, the NZ ME/CFS national advisory society and donations from ME/CFS families (W.P.T, K.P, C.D.E), and from a grant from the Marsden Fund of NZ (E.J.R and A.C). S.S was supported by a doctoral scholarship from the University of Otago (Te Whare Wānanga o Ōtāgo). AC was supported by a Rutherford Discovery fellowship from the Royal Society NZ (Te Apārangi) and currently supported by Sir Charles Hercus Fellowship (from Health Research Council of New Zealand).

Institutional Review Board Statement: The study was conducted in accordance with the Declaration of Helsinki and approved by the Southern Health and Disability Ethics Committee of New Zealand (ethics approval number 17/STH/188 (2018)).

Informed Consent Statement: Informed consent was obtained from all subjects involved in the study.

Data Availability Statement: All datasets generated and analysed during this current study are available in the GEO database NCBI -GSE297189.

Conflicts of Interest: The authors declare no conflict of interest.

References

1. WHO: COVID-19 Cases, World. <https://data.who.int/dashboards/covid19/cases> (2025). Accessed 3 April 2025.
2. Tate WP, Walker MOM, Peppercorn K, Blair ALH, Edgar CD. Towards a Better Understanding of the Complexities of Myalgic Encephalomyelitis/Chronic Fatigue Syndrome and Long COVID. *Int J Mol Sci.* 2023;24(6):5124.
3. Davis HE, McCorkell L, Vogel JM, Topol EJ. Long COVID: major findings, mechanisms and recommendations. *Nature Reviews Microbiology.* 2023:1-14.
4. National Academies of Sciences E, Medicine, Health, Medicine D, Board on Global H, Board on Health Sciences P, et al. A Long COVID Definition: A Chronic, Systemic Disease State with Profound Consequences. In: Goldowitz I, Worku T, Brown L, Fineberg HV, editors. Washington (DC): National Academies Press (US) Copyright 2024 by the National Academy of Sciences. All rights reserved.; 2024.
5. Collins FS: NIH launches new initiative to study "long COVID". <https://www.nih.gov/about-nih/who-we-are/nih-director/statements/nih-launches-new-initiative-study-long-covid> (2021). Accessed 1 April 2025.
6. Staff M. AN OUTBREAK of encephalomyelitis in the Royal Free Hospital Group, London, in 1955. *Br Med J.* 1957;2(5050):895-904.
7. Levine PH, Jacobson S, Pocinki AG, Cheney P, Peterson D, Connelly RR, et al. Clinical, epidemiologic, and virologic studies in four clusters of the chronic fatigue syndrome. *Arch Intern Med.* 1992;152(8):1611-6.
8. Shepherd C, Chaudhuri A, Association M, Association ME, Society ANZM. ME/CFS/PVFS: An Exploration of the Key Clinical Issues. ME Association; 2013.
9. ME-pedia: Millions Missing protests. https://me-pedia.org/wiki/Millions_Missing_protests (2023). Accessed 10th May 2025.
10. Tate W, Walker M, Sweetman E, Helliwell A, Peppercorn K, Edgar C, et al. Molecular Mechanisms of Neuroinflammation in ME/CFS and Long COVID to Sustain Disease and Promote Relapses. *Front Neurol.* 2022;13:877772. doi: 10.3389/fneur.2022.877772.
11. Fang Z, Ahrnsbrak R, Rekito A. Evidence Mounts That About 7% of US Adults Have Had Long COVID. *JAMA.* 2024;332(1):5-6. doi: 10.1001/jama.2024.11370.
12. Xie Y, Choi T, Al-Aly Z. Postacute Sequelae of SARS-CoV-2 Infection in the Pre-Delta, Delta, and Omicron Eras. *N Engl J Med.* 2024;391(6):515-25. doi: 10.1056/NEJMoa2403211.
13. Das S, Taylor K, Kozubek J, Sardell J, Gardner S. Genetic risk factors for ME/CFS identified using combinatorial analysis. *J Transl Med.* 2022;20(1):598. doi: 10.1186/s12967-022-03815-8.
14. Taylor K, Pearson M, Das S, Sardell J, Chocian K, Gardner S. Genetic risk factors for severe and fatigue dominant long COVID and commonalities with ME/CFS identified by combinatorial analysis. *Journal of Translational Medicine.* 2023;21(1):775. doi: 10.1186/s12967-023-04588-4.
15. Gentilotti E, Górska A, Tami A, Gusinow R, Mirandola M, Rodríguez Baño J, et al. Clinical phenotypes and quality of life to define post-COVID-19 syndrome: a cluster analysis of the multinational, prospective ORCHESTRA cohort. *eClinicalMedicine.* 2023;62:102107. doi: <https://doi.org/10.1016/j.eclinm.2023.102107>.
16. Jason LA, Natelson BH, Bonilla H, Sherif ZA, Vernon SD, Verduzco Gutierrez M, et al. What Long COVID investigators can learn from four decades of ME/CFS research. *Brain Behavior and Immunity Integrative.* 2023;4:100022. doi: <https://doi.org/10.1016/j.bbii.2023.100022>.
17. Horwitz LI, Thaweethai T, Brosnahan SB, Cicek MS, Fitzgerald ML, Goldman JD, et al. Researching COVID to Enhance Recovery (RECOVER) adult study protocol: Rationale, objectives, and design. *PLoS One.* 2023;18(6):e0286297. doi: 10.1371/journal.pone.0286297.
18. Komaroff AL, Lipkin WI. Insights from myalgic encephalomyelitis/chronic fatigue syndrome may help unravel the pathogenesis of postacute COVID-19 syndrome. *Trends in Molecular Medicine.* 2021;27(9):895-906. doi: <https://doi.org/10.1016/j.molmed.2021.06.002>.
19. Marshall-Gradisnik S, Eaton-Fitch N. Understanding myalgic encephalomyelitis. *Science.* 2022;377(6611):1150-1. doi: 10.1126/science.abo1261.
20. Komaroff AL: MECFS and Long COVID: Emerging Similarities and Why it Matters. <https://massmecfs.org/news-events/823-mecfs-and-long-covid-emerging-similarities-and-why-it-matters> (2022). Accessed 12 April 2025.

21. Vernon SD, Hartle M, Sullivan K, Bell J, Abbaszadeh S, Unutmaz D, et al. Post-exertional malaise among people with long COVID compared to myalgic encephalomyelitis/chronic fatigue syndrome (ME/CFS). *Work*. 2023;74(4):1179-86. doi: 10.3233/wor-220581.
22. Peppercorn K, Edgar CD, Kleffmann T, Tate WP. A pilot study on the immune cell proteome of long COVID patients shows changes to physiological pathways similar to those in myalgic encephalomyelitis/chronic fatigue syndrome. *Sci Rep*. 2023;13(1):22068. doi: 10.1038/s41598-023-49402-9.
23. Eaton-Fitch N, Rudd P, Er T, Hool L, Herrero L, Marshall-Gradisnik S. Immune exhaustion in ME/CFS and long COVID. *JCI Insight*. 2024;9(20). doi: 10.1172/jci.insight.183810.
24. Helliwell AM, Sweetman EC, Stockwell PA, Edgar CD, Chatterjee A, Tate WP. Changes in DNA methylation profiles of myalgic encephalomyelitis/chronic fatigue syndrome patients reflect systemic dysfunctions. *Clin Epigenetics*. 2020;12(1):167. doi: 10.1186/s13148-020-00960-z.
25. Helliwell AM, Stockwell PA, Edgar CD, Chatterjee A, Tate WP. Dynamic Epigenetic Changes during a Relapse and Recovery Cycle in Myalgic Encephalomyelitis/Chronic Fatigue Syndrome. *Int J Mol Sci*. 2022;23(19). doi: 10.3390/ijms231911852.
26. Brenu EWS, D.R.; Marshall-Gradisnik S.M. . Methylation Profile of CD4+ T Cells in Chronic Fatigue Syndrome/Myalgic Encephalomyelitis. *J Clin Cell Immunol*. 2014;5.
27. de Vega WC, Vernon SD, McGowan PO. DNA methylation modifications associated with chronic fatigue syndrome. *PLoS One*. 2014;9(8):e104757. doi: 10.1371/journal.pone.0104757.
28. de Vega WC, McGowan PO. The epigenetic landscape of myalgic encephalomyelitis/chronic fatigue syndrome: deciphering complex phenotypes. *Epigenomics*. 2017;9(11):1337-40. doi: 10.2217/epi-2017-0106.
29. de Vega WC, Erdman L, Vernon SD, Goldenberg A, McGowan PO. Integration of DNA methylation & health scores identifies subtypes in myalgic encephalomyelitis/chronic fatigue syndrome. *Epigenomics*. 2018;10(5):539-57. doi: 10.2217/epi-2017-0150.
30. Herrera S, de Vega WC, Ashbrook D, Vernon SD, McGowan PO. Genome-epigenome interactions associated with Myalgic Encephalomyelitis/Chronic Fatigue Syndrome. *Epigenetics*. 2018;13(12):1174-90. doi: 10.1080/15592294.2018.1549769.
31. Stockwell PA, Rodger EJ, Gimenez G, Morison IM, Chatterjee A. DMAP2: A Pipeline for Analysis of Whole-Genome-Scale DNA Methylation Sequencing Data. *Curr Protoc*. 2024;4(9):e70003. doi: 10.1002/cpz1.70003.
32. Zhou Y, Zhou B, Pache L, Chang M, Khodabakhshi AH, Tanaseichuk O, et al. Metascape provides a biologist-oriented resource for the analysis of systems-level datasets. *Nat Commun*. 2019;10(1):1523. doi: 10.1038/s41467-019-09234-6.
33. Gopalan S, Carja O, Fagny M, Patin E, Myrick JW, McEwen LM, et al. Trends in DNA Methylation with Age Replicate Across Diverse Human Populations. *Genetics*. 2017;206(3):1659-74. doi: 10.1534/genetics.116.195594.
34. Marcogliese PC, Shashi V, Spillmann RC, Stong N, Rosenfeld JA, Koenig MK, et al. IRF2BPL Is Associated with Neurological Phenotypes. *Am J Hum Genet*. 2018;103(2):245-60. doi: 10.1016/j.ajhg.2018.07.006.
35. Zang W, Zheng X. Structure and functions of cellular redox sensor HSCARG/NMRAL1, a linkage among redox status, innate immunity, DNA damage response, and cancer. *Free Radic Biol Med*. 2020;160:768-74. doi: 10.1016/j.freeradbiomed.2020.09.016.
36. Di Gregoli K, Somerville M, Bianco R, Thomas AC, Frankow A, Newby AC, et al. Galectin-3 Identifies a Subset of Macrophages With a Potential Beneficial Role in Atherosclerosis. *Arterioscler Thromb Vasc Biol*. 2020;40(6):1491-509. doi: 10.1161/atvbaha.120.314252.
37. Kuht HJ, Han J, Maconachie GDE, Park SE, Lee ST, McLean R, et al. SLC38A8 mutations result in arrested retinal development with loss of cone photoreceptor specialization. *Hum Mol Genet*. 2020;29(18):2989-3002. doi: 10.1093/hmg/ddaa166.
38. Yang JY, Deng XY, Li YS, Ma XC, Feng JX, Yu B, et al. Structure of Schlafen13 reveals a new class of tRNA/rRNA- targeting RNase engaged in translational control. *Nat Commun*. 2018;9(1):1165. doi: 10.1038/s41467-018-03544-x.
39. Kanno T, Lin WD, Fu JL, Matzke AJM, Matzke M. A genetic screen implicates a CWC16/Yju2/CCDC130 protein and SMU1 in alternative splicing in *Arabidopsis thaliana*. *Rna*. 2017;23(7):1068-79. doi: 10.1261/rna.060517.116.

40. Dreiza CM, Komalavilas P, Furnish EJ, Flynn CR, Sheller MR, Smoke CC, et al. The small heat shock protein, HSPB6, in muscle function and disease. *Cell Stress and Chaperones*. 2010;15(1):1-11. doi: <https://doi.org/10.1007/s12192-009-0127-8>.
41. Krueger S, Bernhardt A, Kalinski T, Baldensperger M, Zeh M, Teller A, et al. Induction of premalignant host responses by cathepsin x/z-deficiency in *Helicobacter pylori*-infected mice. *PLoS One*. 2013;8(7):e70242. doi: 10.1371/journal.pone.0070242.
42. Kumar CC, Mohan SR, Zavodny PJ, Narula SK, Leibowitz PJ. Characterization and differential expression of human vascular smooth muscle myosin light chain 2 isoform in nonmuscle cells. *Biochemistry*. 1989;28(9):4027-35. doi: 10.1021/bi00435a059.
43. Qin N, Yagel S, Momplaisir ML, Codd EE, D'Andrea MR. Molecular cloning and characterization of the human voltage-gated calcium channel $\alpha(2)\delta$ -4 subunit. *Mol Pharmacol*. 2002;62(3):485-96. doi: 10.1124/mol.62.3.485.
44. Huber C, Mårtensson A, Bokoch GM, Nemazee D, Gavin AL. FGD2, a CDC42-specific exchange factor expressed by antigen-presenting cells, localizes to early endosomes and active membrane ruffles. *J Biol Chem*. 2008;283(49):34002-12. doi: 10.1074/jbc.M803957200.
45. Shen Y, Zhang J, Calarco JA, Zhang Y. EOL-1, the homolog of the mammalian Dom3Z, regulates olfactory learning in *C. elegans*. *J Neurosci*. 2014;34(40):13364-70. doi: 10.1523/jneurosci.0230-14.2014.
46. Apicco DJ, Shlevkov E, Nezich CL, Tran DT, Guilmette E, Nicholatos JW, et al. The Parkinson's disease-associated gene ITPKB protects against α -synuclein aggregation by regulating ER-to-mitochondria calcium release. *Proc Natl Acad Sci U S A*. 2021;118(1). doi: 10.1073/pnas.2006476118.
47. Uchiyama Y, Sakaguchi M, Terabayashi T, Inenaga T, Inoue S, Kobayashi C, et al. Kif26b, a kinesin family gene, regulates adhesion of the embryonic kidney mesenchyme. *Proc Natl Acad Sci U S A*. 2010;107(20):9240-5. doi: 10.1073/pnas.0913748107.
48. Reddy NC, Majidi SP, Kong L, Nemera M, Ferguson CJ, Moore M, et al. CHARGE syndrome protein CHD7 regulates epigenomic activation of enhancers in granule cell precursors and gyrification of the cerebellum. *Nat Commun*. 2021;12(1):5702. doi: 10.1038/s41467-021-25846-3.
49. Lin JX, Leonard WJ. The role of Stat5a and Stat5b in signaling by IL-2 family cytokines. *Oncogene*. 2000;19(21):2566-76. doi: 10.1038/sj.onc.1203523.
50. Kim WS, Weickert CS, Garner B. Role of ATP-binding cassette transporters in brain lipid transport and neurological disease. *J Neurochem*. 2008;104(5):1145-66. doi: 10.1111/j.1471-4159.2007.05099.x.
51. Dib S, Pahnke J, Gosselet F. Role of ABCA7 in Human Health and in Alzheimer's Disease. *Int J Mol Sci*. 2021;22(9). doi: 10.3390/ijms22094603.
52. Steagall RJ, Rusiñol AE, Truong QA, Han Z. HSPA12B is predominantly expressed in endothelial cells and required for angiogenesis. *Arterioscler Thromb Vasc Biol*. 2006;26(9):2012-8. doi: 10.1161/01.ATV.0000235720.61091.c7.
53. Carruthers BM, Jain AK, De Meirleir KL, Peterson DL, Klimas NG, Lerner AM, et al. Myalgic Encephalomyelitis/Chronic Fatigue Syndrome. *Journal of Chronic Fatigue Syndrome*. 2003;11(1):7-115. doi: 10.1300/J092v11n01_02.
54. WHO: A clinical case definition of post COVID-19 condition by a Delphi consensus, 6 October 2021. https://www.who.int/publications/i/item/WHO-2019-nCoV-Post_COVID-19_condition-Clinical_case_definition-2021.1 (2021). Accessed.
55. Peppercorn K, ; Edgar, C.; Al Momani, S.; Rodger, E. J.; Tate, W.P.; Chatterjee, A. Application of DNA methylome analysis to patients with ME/CFS. *Methods in Molecular Biology*. in press: Springer; 2025.
56. Ludgate JL, Wright J, Stockwell PA, Morison IM, Eccles MR, Chatterjee A. A streamlined method for analysing genome-wide DNA methylation patterns from low amounts of FFPE DNA. *BMC Med Genomics*. 2017;10(1):54. doi: 10.1186/s12920-017-0290-1.
57. Rodger EJ, Stockwell PA, Almomani S, Eccles MR, Chatterjee A. Protocol for generating high-quality genome-scale DNA methylation sequencing data from human cancer biospecimens. *STAR Protoc*. 2023;4(4):102714. doi: 10.1016/j.xpro.2023.102714.
58. Stockwell PA, Chatterjee A, Rodger EJ, Morison IM. DMAP: differential methylation analysis package for RRBS and WGBS data. *Bioinformatics*. 2014;30(13):1814-22. doi: 10.1093/bioinformatics/btu126.

59. Chatterjee A, Stockwell PA, Rodger EJ, Morison IM. Comparison of alignment software for genome-wide bisulphite sequence data. *Nucleic Acids Res.* 2012;40(10):e79. doi: 10.1093/nar/gks150 10.1093/nar/gks150. Epub 2012 Feb 16.

Disclaimer/Publisher's Note: The statements, opinions and data contained in all publications are solely those of the individual author(s) and contributor(s) and not of MDPI and/or the editor(s). MDPI and/or the editor(s) disclaim responsibility for any injury to people or property resulting from any ideas, methods, instructions or products referred to in the content.